

## Dynamic thermal model development of direct methanol fuel cell

Mohammad Biswas<sup>a</sup>, Tabbi Wilberforce<sup>b,\*</sup>

<sup>a</sup> The University of Texas at Tyler, Department of Mechanical Engineering, 3900 University Blvd, 75799, Tyler, Tx United States of America

<sup>b</sup> Mechanical Engineering and Design, Aston University, School of Engineering and Applied Science, Aston Triangle, B4 7ET, Birmingham, United Kingdom

### ARTICLE INFO

#### Keywords:

Direct methanol fuel cell (DMFC)  
Artificial neural network  
Temperatures  
Learning algorithms

### ABSTRACT

Direct methanol fuel cell (DMFC) is fueled with liquid methanol coupled with air to produce power at reasonably lower operational conditions while resulting in by-products of carbon dioxide and water, which is more environmentally friendly. Due to the complexity associated with the performance of direct methanol fuel cell, the application of artificial neural network (ANN) can significantly predict the characteristic performance of the cells. Nevertheless, limited studies have delved into the exploration of artificial neural network in the prediction of the transient characteristics of direct methanol fuel cells. The current study however presents a detailed investigation into the prediction of the dynamic thermal characteristics of a direct methanol fuel cell stack subjected to varying operational environment. Parameters considered in the study as input include methanol concentration, anode as well as cathode inlet flow rates, coupled with current. Outcomes for the artificial neural network models for three varying learning algorithms were ascertained for anode and cathode temperatures, which were forecasted closely by models with higher number of hidden neurons. Such models have coefficients of determination of 0.95 or more and mean square error less than 0.04. Thus, the outcome of the study presents prospects for artificial neural network methods as optimum control approach in direct methanol fuel cell development.

### 1. Introduction

Given the current direction of greener energy demand to curb global warming effects, there has been significant amount of research conducted to find an alternative to fossil fuel-based energy systems [1–4]. The need for the sudden change is due to the accelerated depletion of fossil reserves and the harmful effect of fossil commodities on the environment [5,6]. Other factors attributed to the sudden drift for a more sustainable means of harnessing energy is due to unstable prices of fossil product on the world market. Renewable energy is projected by the research community as possible replacement for fossil products [7, 8]. The main limitations associated to conversional means of harnessing energy from renewable sources are intermittency and initial capital cost required in generating energy via this means. Fuel cells, an energy converting device is however one of the projected renewable sources of energy receiving lots of media attention from the research community because they are environmentally friendly [9–11]. There are different types of fuel cells and each of them differ based on several factors like the type of membrane used in the development of the cell and their general operating conditions [12]. One alternative considered to benefit

the environment and help in green technology development is direct methanol fuel cell (DMFC) [13]. The cell is capable of providing power to a load in an application while minimizing environmental effect. This electrochemical energy converting unit utilizes liquid methanol solution as fuel. The chemical energy in the fuel undergoes a transformation to electrical energy. However, the main by-products are carbon dioxide as well as water, thus minimal potential hazard to the atmosphere. This is a significant improvement compared to conversional energy generating units powered by fossil commodities. There is a direct correlation between direct methanol fuel cell and proton exchange membrane fuel cells as both electrochemical devices functions at relatively low temperatures. The only difference is for proton exchange membrane fuel cells, the fuel used is hydrogen unlike DMFC where methanol is utilized. However, direct methanol fuel cell can be more advantageous than PEMFC in different applications because no reformer is needed to produce hydrogen since liquid methanol is a direct reactant. It must however be highlighted that the energy density of methanol, which is 15.9 MJ/L, outweighs that of hydrogen under pressurized conditions, which is 1.9 MJ/L at a pressure of 20 MPa for example [13]. In terms of safety, methanol can be stored under safer conditions compared to hydrogen

\* Corresponding author.

E-mail address: [t.wotwe@aston.ac.uk](mailto:t.wotwe@aston.ac.uk) (T. Wilberforce).

<https://doi.org/10.1016/j.ijft.2023.100294>

Available online 27 January 2023

2666-2027/© 2023 The Author(s). Published by Elsevier Ltd. This is an open access article under the CC BY-NC-ND license (<http://creativecommons.org/licenses/by-nc-nd/4.0/>).

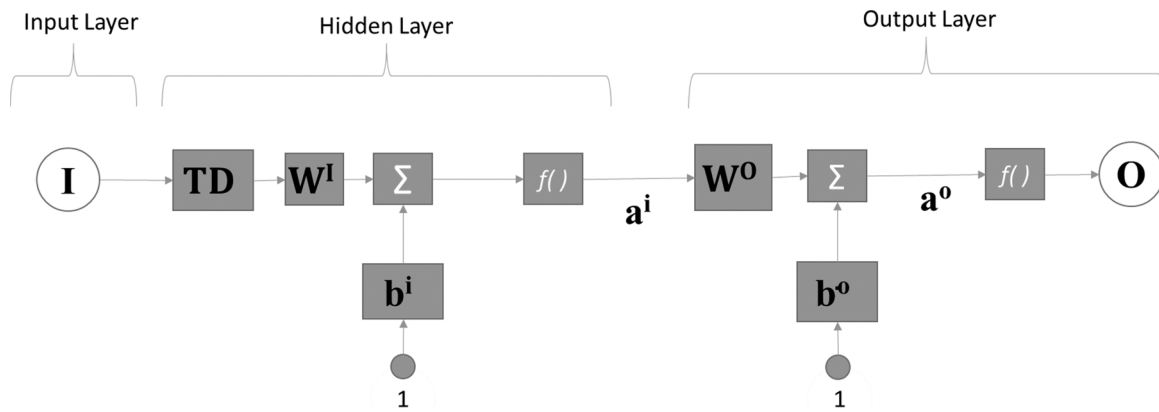


Fig. 1. Neural network model.

which in the past has recorded some unfortunate life-threatening events like the Hindenburg disaster [13,14]

For consistent operation of DMFC systems, thermal and power management is vital in optimal and efficient performance under dynamic operating conditions. For example, thermal and water management is critical to ensure the DMFC is not dehydrated due to possible excessive water loss at high cathode flow rates and temperatures, nor flooded due to excessive water retained due to low anode and cathode flow rates and temperatures, to maintain optimal DMFC cell performance [15]. To circumvent expensive trial-and-error approaches, many studies are being conducted to develop and simulate multiple input and multiple output variable techniques to estimate direct methanol thermal characteristics subjected to varying operational environments. Despite the fact that there are several methods including empirical regression and semi-analytical approach to develop such dynamic models, artificial neural network (ANN) technique has hardly been utilised for DMFC applications, even though its potential can be seen in studies of other fuel cells [15–18]. There has been remarkable technological advancement in the implementation of ANN for varying purposes including energy conversion systems. This modeling technique is capable of managing all complexity associated with engineering systems. For varying input as well as output parameters, the model is able to present nonlinear transient characteristics of most engineering systems. The margin for error is very small and the solution can easily converge within a limited period of time unlike traditional statistical methods like the nonlinear regression models [19–21]. Artificial Neural Network are categorized into various types subject to their application but the time-series ANN modeling with three different learning algorithms for such dynamic empirical modeling approach seem the most suitable in energy conversion system applications.

In this study, ANN modeling is carried out for comparing accuracy in prediction of DMFC thermal transient characteristics for different learning algorithms. Thermal model of DMFC includes the prediction of inlet and outlet temperatures of the fluid flow across the DMFC channels through empirical modeling approach using ANN, which can be used in temperature and flow control strategy to improve water and thermal management of the DMFC system for higher efficiency performance. The thermal models obtained are varied by the different algorithms and hidden neurons in ANN with a conventional structure. The study is systematized as follows: The first part of the study captures an introduction of the topic on dynamic DMFC modeling using ANN, Section 2 describes the experimental setup as well as explains and illustrates the ANN and its associated learning algorithms, the third section of the study presents the outcome of the experiment conducted as well as model results along with a discussion of these results to summarize the outcome of the investigation and, finally, Section 4 provides the concluding points of the study.

## 2. Methodology

The development of artificial neural network could be likened to the nervous system of a human that is modelled mathematically. The evolution of artificial neural network can be traced to over half a century ago. The applications of the concept have widened in the last couple of years because of substantial progress marked in solving advanced problems using latest technology. Solutions for most of these thought-provoking technical issues are deduced within a limited period with high computational capability [22,23].

Fig. 1 captures a dynamic neural network with time delay only structure made up of an input variable vector that is considered to be independent, a hidden layer of neurons with time delay, weight and bias matrices, as well as an output layer. The neuron is linked to another neuron via weight function  $w$  but the response vectors  $a^i$  and  $a^o$  are generated by the activation function  $f()$ . Similarly, it is worth noting that the neuron number may vary autonomously. The neurons in succeeding layers obtain response of the previous layer. Fig. 1 shows a model that has input  $I$ , which accounts for all input variables, while the output layer of output vector  $O$ , which considers the output variable. The performance of summation coupled with the application of activation functions to deduce hidden output layer values for one time step ahead occurs due to the composition of the ANN model. The activation function for hidden layer is taken as linear function while activation function for output layer is log-sigmoid function.

To train and validate the models, the experimental data obtained from a fuel cell test station at the University of Florida was utilised [15]. The experimental setup included a DMFC stack, which were assembled and conditioned at the University of Florida laboratory facilities. The cell stack was made up of 4 air-breathing direct methanol fuel cell architecture single cells with passive cathode water recovery [24–26]. The experimental hardware is connected to a computer using LabVIEW® and corresponding National Instrument input-output boards as an interface for the purposes of acquiring data at a sampling frequency of 1–50 Hz and adjusting the input signals, the cell current density and the cathode air-flow rate. Thus, the primary input variables used were current density in mA/cm<sup>2</sup>, anode and cathode inlet flow rates (in SLPM or L/min) and temperatures (in °C) while the key outputs captured for thermal characteristics prediction were anode and cathode outlet temperatures in °C. The various cell components were developed by the team of researchers at the University of Florida. With the test station in place, testing of the cell for varying step changes of input variable such as air flow rate in SLPM was carried out. Data acquisition for dynamic analysis of the fuel cell [27] was executed with the aid of LabVIEW® software coupled with National Instruments [28] boards. The procedure involves the startup of the DMFC unit to reach stable and consistent operation for a given temperature and flow rate. Further detailed information pertaining to the fuel cell test station procedures could be harnessed from

**Table 1**  
Statistical analysis of model results for anode outlet temperature.

ANN learning algorithms	Number of hidden neurons	Coefficient of determination	Mean squared error
LM	1	0.961	0.295
LM	10	0.983	0.128
LM	20	0.993	0.055
LM	30	0.994	0.043
LM	40	0.996	0.028
SCG	1	0.956	0.337
SCG	10	0.978	0.167
SCG	20	0.971	0.222
SCG	30	0.978	0.164
SCG	40	0.959	0.316
Bayesian	1	0.961	0.294
Bayesian	10	0.993	0.055
Bayesian	20	0.995	0.036
Bayesian	30	0.997	0.027
Bayesian	40	0.997	0.024

**Table 2**  
Statistical analysis of model results for cathode outlet temperature.

ANN structure	Number of hidden neurons	Coefficient of determination	Mean squared error
LM	1	0.975	0.196
LM	10	0.986	0.109
LM	20	0.971	0.231
LM	30	0.983	0.137
LM	40	0.989	0.090
SCG	1	0.951	0.403
SCG	10	0.984	0.128
SCG	20	0.982	0.140
SCG	30	0.936	0.501
SCG	40	0.987	0.102
Bayesian	1	0.977	0.178
Bayesian	10	0.996	0.035
Bayesian	20	0.997	0.023
Bayesian	30	0.997	0.020
Bayesian	40	0.998	0.016

[13,27].

During the training process, output values are deduced subject to the input parameters, but this only occurs provided the input variables are fed to ANN. Evaluation of every pattern within the network highlights the fact that the input parameters are utilized to deduce the output. There is then a comparison between the trained pattern and output for consistency as well as to reduce the error margin. In the event that the error margin is significantly high, the model can be made to process all input parameters again till the error meet conditions laid out. For the completion of the training process, the ANN should maintain estimated weight as well as the bias value for the validation process based on dedicated validation parameters. Identification of patterns coupled with specific decision-making process is then carried out using untrained input parameters subject to the overall aim for the model development. The utmost goal is reducing the error margin between the experimental parameters and the predicted values. There are several approaches that can be adopted in ensuring the error margin between the two values is reduced significantly, but this is subject to the discretion of the operator. An example for this approach includes mean squared error (MSE). The mean squared error can be described as

$$MSE = \frac{1}{n} \sum (Z - Y)^2 \quad (1)$$

Occurrence for the data points is  $n$  while the values predicted is  $Z$ . Experimental data is denoted as  $Y$  [19]. The errors are applicable in other statistical studies like coefficient of determination. Eq. (2) captures a mathematical representation for the coefficient of determination

$$R^2 = [Cor(Z, Y)]^2 = 1 - \frac{\sum (Z - Y)^2}{\sum (Y - \bar{Y})^2} \quad (2)$$

Correlation coefficient is denoted as  $Cor(Z, Y)$ . The average value for the data is represented as  $\bar{Y}$  while sum of square is  $\sum (Y - \bar{Y})^2$  [20].

The variation for  $R^2$  is often between 0 – 1. For the coefficient of determination being 0.95, it implies that 95 percent of variability is captured by the predictor parameters, which is ideal for excellent fit. Attaining a suitable model is equally dependent on training speed coupled with reduction in the margin of error but optimizing the model is equally important. For fast convergence, the Newton's method

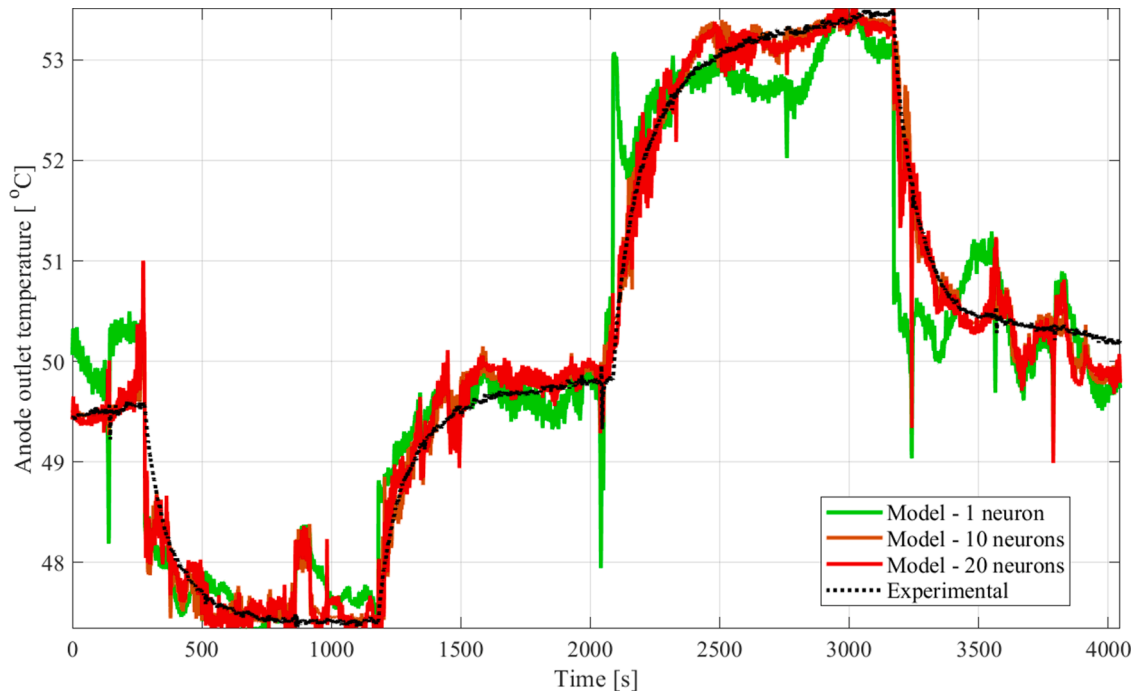


**Fig. 2.** Data from experiment coupled with model responses for anode outlet temperature using ANN with LM algorithm.

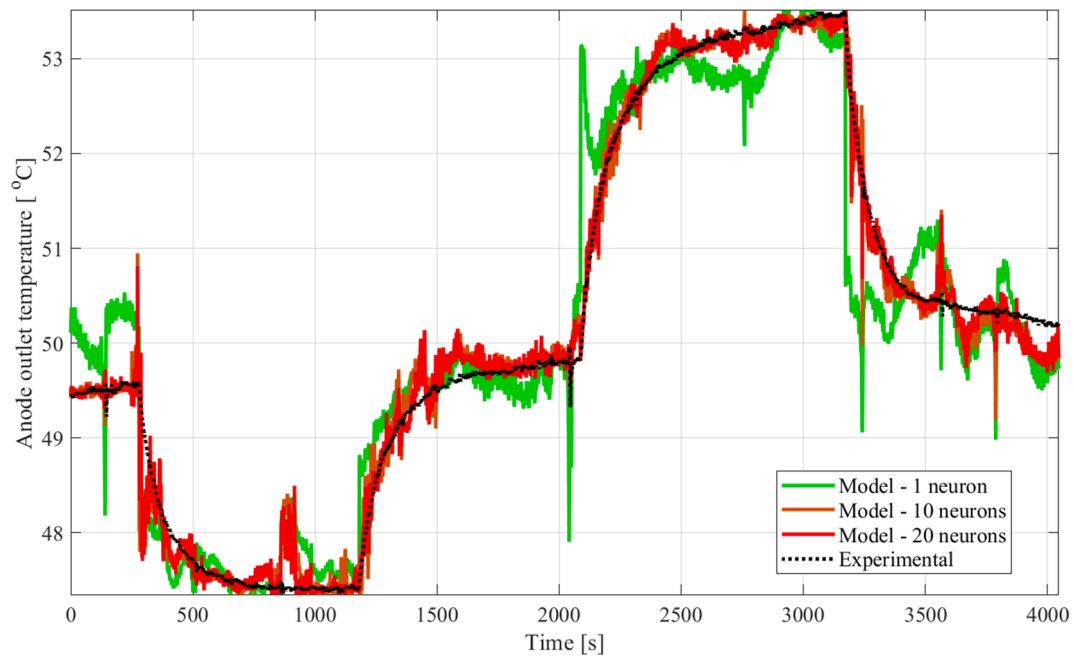


Fig. 3. Data from experiment coupled with model responses for anode outlet temperature using ANN with Bayesian based algorithm.

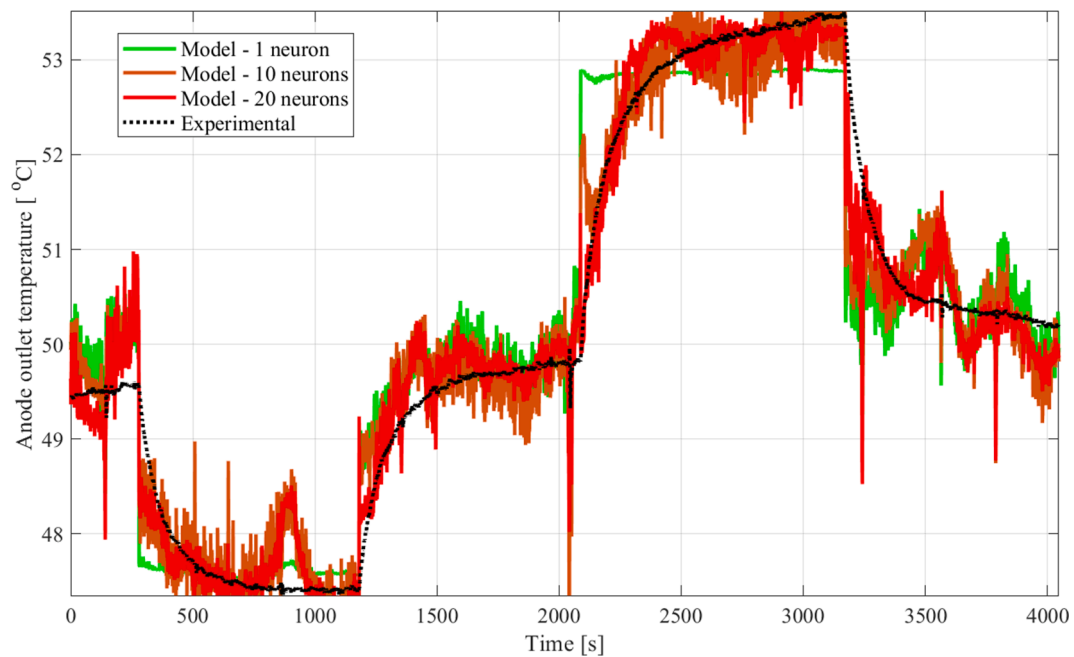


Fig. 4. Data from experiment coupled with model responses for anode outlet temperature using ANN with SCG algorithm.

application to train the ANN is desired, but, for the entire network, the Hessian matrix (HM) is singular [29]. The Levenberg-Marquardt (LM) algorithm is a substitute to the Hessian matrix that is capable of resolving issues pertaining to the Hessian matrix. In the Levenberg-Marquardt (LM) algorithm, there is an addition of a term  $\mu I$  to HM. This process is done for enhancing conditioning. Detailed investigations have been executed to ascertain suitable values for  $\mu$  [30]. When  $\mu$  values are smaller, model performance approaches Newton's algorithm. In the case of a large  $\mu$  values, there is a higher gradient descent. A neural network model is captured in Fig. 1.

Scaled conjugate gradient (SCG) method from study by Moller [25], is prefaced on conjugate directions, however unlike other conjugate gradient algorithms, this methodology doesn't execute a line search at

each iteration, whereas other conjugate gradient algorithms do require linear search for every iteration [25]. This raises computational cost of the system. SCG was constructed to remove the necessity to perform tedious line searches. When using the scaled conjugate gradient approach, the MATLAB® training function 'trainscg' revises weight as well as the bias parameter of network during the training process. Training of a specific network may occur provided there is a derivative function for the weights as well as the transfer functions. Step size in the scaled conjugate gradient method is function of a quadratic approximation for error function. This ensures there is robustness as well as independency for the values presented by the user. The step size is approximating with the aid of varying methods. Second order term deduced from Eq. (3):

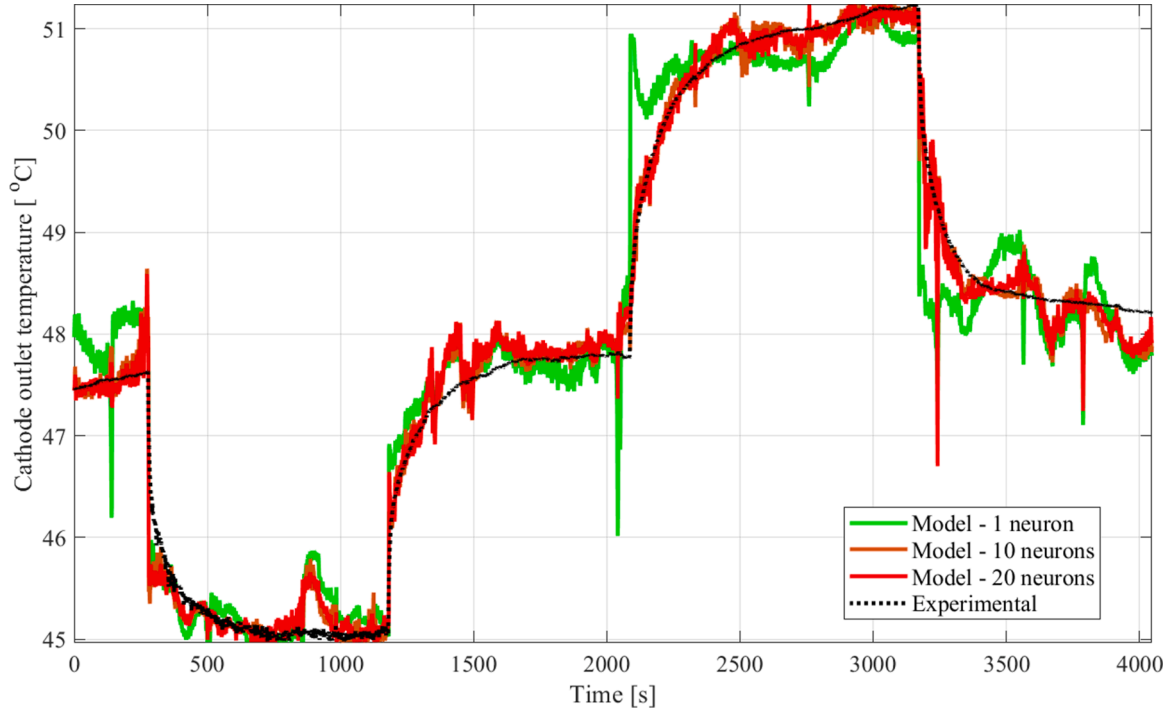


Fig. 5. Experimental and model responses of cathode outlet temperature using ANN with LM algorithm.

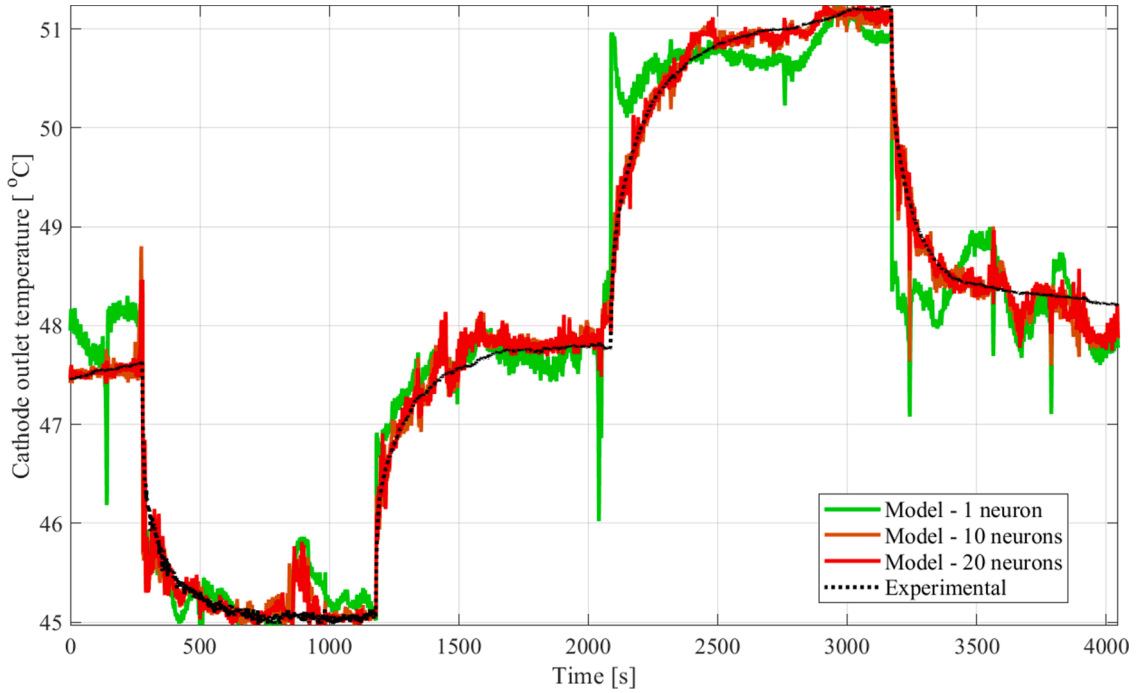


Fig. 6. Experimental and model responses of cathode outlet temperature using ANN with Bayesian based algorithm.

$$\bar{\sigma}_k = \frac{E'(\bar{\omega}_k + \sigma_k \bar{p}_k) - E'(\bar{\omega}_k)}{\sigma k} + \lambda_k \bar{p}_k \tag{3}$$

$\lambda_k$  is denoted as a scalar unit and changes based on the sign of  $\sigma k$ .

$$\alpha_k = \frac{\mu_k}{\delta_k} = \frac{-\bar{p}_j^T E'_{q\omega}(\bar{y}_1)}{\bar{p}_j^T E''(\bar{\omega}) \bar{p}_j} \tag{4}$$

where  $\bar{\omega}$  is denoted as the vector in space  $R^n$ ,  $E\bar{\omega}$  is the global error

function,  $E'\bar{\omega}$  is gradient of error,  $E'_{q\omega}(\bar{y}_1)$  is quadratic approximation, and  $\bar{p}_1, \bar{p}_2, \dots, \bar{p}_k$  weight vectors that are not zero.

$\lambda_k$  can equally be revised using Eq. (5)

$$\bar{\lambda}_k = 2 \left( \lambda_k - \frac{\delta_k}{|p_k^2|} \right) \tag{5}$$

When  $\Delta_k > 0.75$ , then  $\lambda_k = \frac{\lambda_k}{4}$

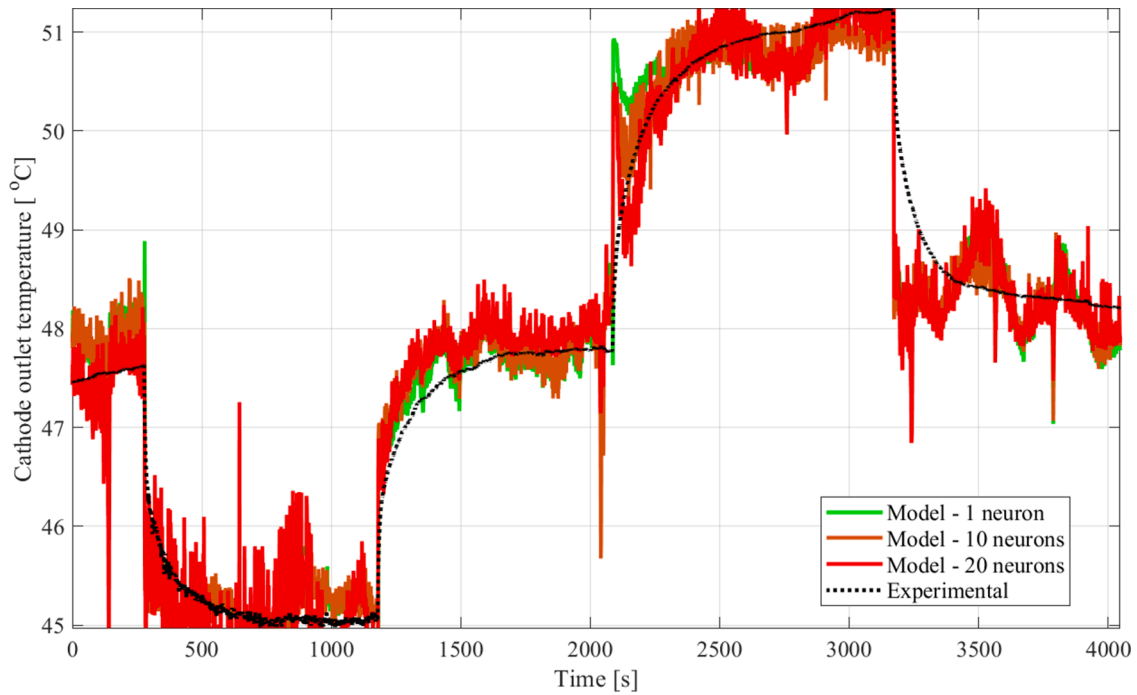


Fig. 7. Experimental and model responses of cathode outlet temperature using ANN with SCG algorithm.

$$\Delta_k < 0.25, \text{ then } \lambda_k = \lambda_k + \frac{\delta_k(1 - \Delta_k)}{|p_k^2|}$$

$\Delta_k$  is a comparative value and deduced using Eq. (6).

$$\Delta_k = \frac{2\delta_k[E(\bar{w}_k) - E(\bar{w}_k + \alpha_k \bar{p}_k)]}{\mu_k^2} \quad (6)$$

The Bayesian estimation and regularization entails a Hessian matrix. For Mean square error, cost function as well as regularization by summation of weights highlights the fact that Hessian matrix is quadratic hence deduced using LM [26]. Eq. (7) denotes the objective function:

$$F = \alpha E_w + \beta E_D \quad (7)$$

For the Bayesian framework, weight related to the network are seen as variables arbitrarily chosen. Eq. (8) is the probability function for an array  $w$  of network weights

$$f(w|D, \alpha, \beta, M) = \frac{f(D|w, \beta, M)f(w|\alpha, M)}{f(D|\alpha, \beta M)} \quad (8)$$

$M$  symbolizes the neural network model utilized while  $f(w|\alpha, M)$  is the prior density.  $f(D|w, \beta, M)$  this is the likelihood function.

### 3. Results and discussions

Fitting of the model was carried out using MATLAB Neural Network Toolbox®. Five inputs were considered for the study while two output variables were equally taken into account in the investigation [31]. The developed models utilised >90% of over 4000 data sets for training, <5% to test and validate the model. There was variation between the number of hidden layer neurons within single hidden layer in order to determine the best fit model. Table 1 presents a comparison between the mean squared error and the  $R^2$  using 3 algorithms for the outlet temperature at the anode. Type of algorithm is captured in column 1 while varying ranges of the hidden neurons are presented in column 2. The  $R^2$  are in column 3 while the mean squared error is presented in column 3. Similar to Table 1 and Table 2 presents a comparison between the mean squared error and  $R^2$  for cathode outlet temperature. Fig. 2 shows experimental and model responses of the anode outlet temperature

where the ANN models with LM are of 1, 10 and 20 hidden neurons. The y-axis is outlet temperature in °C while x-axis is time in s. Fig. 3 includes plots of experimental and model responses of the anode outlet temperature where the ANN models with Bayesian algorithm are of 1, 10 and 20 hidden neurons. Fig. 4 shows plots of experimental and model responses of the anode outlet temperature where the ANN models with SCG algorithm are of 1, 10 and 20 hidden neurons.

Fig. 5 compares the experimental and model responses of ANN model with LM for cathode outlet temperature. Fig. 6 includes plots of experimental and model responses of the cathode outlet temperature where the ANN models with Bayesian regularization of 1, 10 and 20 hidden neurons. Fig. 7 shows the model responses of ANN model with SCG for cathode outlet temperature against the response of the experimental data.

From all tables and figures, it can be seen that most models of different number of hidden neurons can effectively approximate the transient DMFC temperature data. However, models with higher number of hidden neurons (higher than 20) for all three algorithms perform better from the mean squared error values as well as  $R^2$  values. Moreover, Bayesian regularization algorithm consistently predicts more accurately for anode and cathode outlet temperatures compared to the other algorithms for very high hidden neurons such as at 40 hidden neurons.

Although there are several investigations conducted on fuel cells especially for DMFCs [32–34], there are a handful of research work in estimating dynamic thermal behavior. One of the few studies includes the development of an adaptive fuzzy neural networks control of DMFC stack temperature. For this study, dynamic temperature models with the aid of radial basis function artificial neural network were developed [17, 35]. There was a perfect correlation between the developed model and the experimental data. The outcome of the investigation highlights the fact that the temperature response could be maintained at ideal temperature range using the developed controller. Similarly, other methods using artificial neural network for the prediction of dynamic voltage as well as thermal characteristics of different types of fuel cells have equally been presented. For instance, dynamic proton exchange membrane fuel cell stack model with the aid of recurrent neural network was carried out [16]. The authors used two varying artificial neural networks

in their investigation. The model was established with the aid of actual load data for demonstrating good correlation with the gathered data where their eXogenous and nonlinear output error models forecasted voltage of the cell with error lower than 2%. Thus, the results obtained from the models presented in this paper for DMFC are comparable to the results of the data and studies found in literature for mainly PEMFC. Although there are a handful of relevant studies on DMFC modeling using ANN, there are not any studies like this to compare to that could be found.

#### 4. Conclusion

In summary, the present investigation explored a comparison between the utilization of artificial neural network modeling method for varying learning algorithms on a DMFC. The models are comparable and consistent with the empirical data. Although most dynamic ANN model responses had high coefficients of determinations (greater than 0.93), artificial neural network model using any of three algorithms with higher number of hidden neurons showed the best fit. So, it can however be argued that dynamic artificial neural network with higher number of hidden neurons (>20) combined with Bayesian regularization algorithm will have better performance when implementations of such models are made for optimization of related control design in thermal management of DMFC systems. For example, the optimal ANN model to estimate the anode outlet temperature used Bayesian algorithm and 40 neurons to result in mean square error of only 0.024 and coefficient of determination of 0.997. Similarly, the most optimal ANN model to estimate the cathode outlet temperature also involved Bayesian algorithm and about 40 neurons to result in mean square error of only 0.016, which is the lowest error from the data collected, and coefficient of determination of 0.998. Moreover, majority of these modeling techniques remain valuable tools in building a control architecture for similar systems to enhance efficiency as well as ensure stabilization of operation for real-time transient conditions. The optimized models of outlet temperatures for the DMFC using artificial neural network can be used to develop such control architecture to improve water and thermal management to thus consequently in reduce parasitic power consumption and improve DMFC performance efficiency.

#### Declaration of Competing Interest

The authors declare that they have no known competing financial interests or personal relationships that could have appeared to influence the work reported in this paper.

#### Data availability

Data will be made available on request.

#### References

- [1] Bakartxo Egilegor, Hussam Jouhara, Josu Zuazua, Fouad Al-Mansour, Kristijan Plesnik, Luca Montorsi, Luca Manzini, ETEKINA: analysis of the potential for waste heat recovery in three sectors: aluminium low pressure die casting, steel sector and ceramic tiles manufacturing sector, *Int. J. Thermofluids* 1–2 (2020), 100002, <https://doi.org/10.1016/j.ijft.2019.100002>. VolumeISSN 2666-2027.
- [2] Daniel Brough, João Ramos, Bertrand Delpech, Hussam Jouhara, Development and validation of a TRNSYS type to simulate heat pipe heat exchangers in transient applications of waste heat recovery, *Int. J. Thermofluids* 9 (2021), <https://doi.org/10.1016/j.ijft.2020.100056>. Article 100056ISSN 2666-2027.
- [3] Borbala Rebeka David, Sean Spencer, Jeremy Miller, Sulaiman Almahmoud, Hussam Jouhara, Comparative environmental life cycle assessment of conventional energy storage system and innovative thermal energy storage system, *Int. J. Thermofluids* 12 (2021), 100116, <https://doi.org/10.1016/j.ijft.2021.100116>. VolumeISSN 2666-2027.
- [4] Magdi Rashad, Navid Khordehghah, Alina Żabnieńska-Góra, Lujean Ahmad, Hussam Jouhara, The utilisation of useful ambient energy in residential dwellings to improve thermal comfort and reduce energy consumption, *Int. J. Thermofluids* 9 (2021), 100059, <https://doi.org/10.1016/j.ijft.2020.100059>. VolumeISSN 2666-2027.
- [5] Daniel Hill, Adam Martin, Nathanael Martin-Nelson, Charles Granger, Matthew Memmott, Kody Powell, John Hedengren, Techno-economic sensitivity analysis for combined design and operation of a small modular reactor hybrid energy system, *Int. J. Thermofluids* 16 (2022), 100191, <https://doi.org/10.1016/j.ijft.2022.100191>. VolumeISSN 2666-2027.
- [6] Ammar Alkhalidi, Khalid Alqarra, Mohammad Ali Abdelkareem, A.G. Olabi, Renewable energy curtailment practices in Jordan and proposed solutions, *Int. J. Thermofluids* 16 (2022), 100196, <https://doi.org/10.1016/j.ijft.2022.100196>. VolumeISSN 2666-2027.
- [7] Ammar Alkhalidi, Tuqa Alrousan, Manal Ishbeyhat, Mohammad Ali Abdelkareem, A.G. Olabi, Recommendations for energy storage compartment used in renewable energy project, *Int. J. Thermofluids* 15 (2022), 100182, <https://doi.org/10.1016/j.ijft.2022.100182>. VolumeISSN 2666-2027.
- [8] Hussam Jouhara, Alina Żabnieńska-Góra, Navid Khordehghah, Darem Ahmad, Tom Lipinski, Latent thermal energy storage technologies and applications: a review, *Int. J. Thermofluids* 5–6 (2020), 100039, <https://doi.org/10.1016/j.ijft.2020.100039>. VolumeISSN 2666-2027.
- [9] Abdelnasir Omran, Alessandro Lucchesi, David Smith, Abed Alaswad, Amirpiran Amiri, Tabbi Wilberforce, José Ricardo Sodré, A.G. Olabi, Mathematical model of a proton-exchange membrane (PEM) fuel cell, *Int. J. Thermofluids* 11 (2021), 100110, <https://doi.org/10.1016/j.ijft.2021.100110>. VolumeISSN 2666-2027.
- [10] F.N. Khatib, Tabbi Wilberforce, James Thompson, A.G. Olabi, Experimental and analytical study of open pore cellular foam material on the performance of proton exchange membrane electrolyzers, *Int. J. Thermofluids* 9 (2021), <https://doi.org/10.1016/j.ijft.2021.100068>. Article 100068.
- [11] Tabbi Wilberforce, Imran Muhammad, Dynamic modelling and analysis of organic Rankine cycle power units for the recovery of waste heat from 110 kW proton exchange membrane fuel cell system, *Int. J. Thermofluids* 17 (2023), 100280, <https://doi.org/10.1016/j.ijft.2023.100280>. VolumeISSN 2666-2027.
- [12] Ahmad Baroutaji, Arun Arjunan, Mohamad Ramadan, John Robinson, Abed Alaswad, Mohammad Ali Abdelkareem, Abdul-Ghani Olabi, Advancements and prospects of thermal management and waste heat recovery of PEMFC, *Int. J. Thermofluids* 9 (2021), 100064, <https://doi.org/10.1016/j.ijft.2021.100064>. VolumeISSN 2666-2027.
- [13] M.A.R. Biswas, "Model development and control design of fuel cell systems to power portable devices," 2013.
- [14] R. O'hayre, S. Cha, W. Colella, F. Prinz, *Fuel Cell Fundamentals*, 3 ed., Wiley, New York, 2005.
- [15] M.A.R. Biswas, S. Mudiraj, W. Lear, O. Crisalle, Systematic approach for modeling methanol mass transport on the anode side of direct methanol fuel cells, *Int. J. Hydrogen Energy* 39 (15) (2014) 8009–8025.
- [16] F.d.C. Lopes, E.H. Watanabe, L.G.B. Rolim, Analysis of the time-varying behavior of a PEM fuel cell stack and dynamical modeling by recurrent neural networks, in: *Brazilian Power Electronics Conference (COBEP 2013)*, Gramado, 2013.
- [17] Q. Miao, G.-y. Cao, X.-j. Zhu, Performance analysis and fuzzy neural networks modeling of direct methanol fuel cell, *J. Shanghai Univ. (English Edition)* 11 (2007) 84–87.
- [18] L. Xu, J. Xiao, Dynamic modeling and simulation of PEM fuel cells based on BP neural network, in: *Intelligent Systems and Applications (ISA), 2011 3rd International Workshop on*, 2011.
- [19] M.T. Hagan, H.B. Demuth, M.H. Beale, *Neural Network Design*, PWS Publishing Company, Boston, 1996.
- [20] J. Henken, M.A.R. Biswas, Validation of neural network model for residential energy consumption, in: *2015 ASEE-GSW Annual Conference*, San Antonio, 2015.
- [21] M. Tafazoli, H. Baseri, E. Alizadeh, M. Shakeri, Modeling of direct methanol fuel cell using the artificial neural network, *J. Fuel Cell Sci. Technol.* 10 (4) (2013), 041007.
- [22] M.A.R. Biswas, M.D. Robinson, N. Fumo, Prediction of residential building energy consumption: a neural network approach, *Energy* 117 (2016) 84–92.
- [23] M.D. Robinson, M.T. Manry, Two-Stage second order training in feedforward neural networks, in: *The Twenty-Sixth International FLAIRS Conference*, St. Pete Beach, 2013.
- [24] A. Mossman and D. Olmeijer, "Composite polymer electrolyte membranes". United States of America Patent 12/031,675, #feb#~14 2008.
- [25] Møller Martin Fodsette, A scaled conjugate gradient algorithm for fast supervised learning, *Neural Netw.* 6 (4) (1993) 525–533, [https://doi.org/10.1016/S0893-6080\(05\)80056-5](https://doi.org/10.1016/S0893-6080(05)80056-5). VolumeISSN 0893-6080.
- [26] A. Mossman, B. Wells, R. Barton and H. Voss, "Passive recovery of liquid water produced by fuel cells". United States of America Patent 11/936,048, #nov#~6 2007.
- [27] Fuel Cell Technologies., "Fuel cell test station," Albuquerque, 2017.
- [28] National Instruments, "LabVIEW," Austin, TX, 2008.
- [29] J. Wille, On the structure of the Hessian matrix in feedforward networks and second derivative methods, in: *International Conference on Neural Networks*, Houston, 1997.
- [30] Jr. J. E. D., R.B. Schnabel, *Numerical Methods for Unconstrained Optimization and Nonlinear Equations*, Soc. for Industrial & Applied Math, Philadelphia, 1996.
- [31] MATLAB, Version 8.5 (R2015a), The MathWorks Inc, Natick, Massachusetts, 2015.
- [32] H.S. Pajaei, S. Abbasian, B. Mehdizadeh, Prediction of direct methanol fuel cell using artificial neural network, *Asian J. Chem.* 24 (11) (2012) 5413–5414.

- [33] M.A.R. Biswas, M.D. Robinson, Performance estimation of direct methanol fuel cell using artificial neural network, in: ASME 2015 International Mechanical Engineering Congress and Exposition, 2015.
- [34] K.-Y. Chang, C.-Y. Chang, W.-J. Wang, C.-Y. Chen, Modeling polarization of a dmfc system via neural network with immune-based particle swarm optimization, *Int. J. Green Energy* 9 (4) (2012) 309–321.
- [35] Q. Miao, G.-y. Cao, X.-j. Zhu, Nonlinear modeling based on RBF neural networks identification and adaptive fuzzy control of DMFC stack, *Journal of Shanghai University (English Edition)* 10 (4) (2006) 346–351.